

Fabrication and microwave absorbing properties of $\text{Li}_{0.35}\text{Zn}_{0.3}\text{Fe}_{2.35}\text{O}_4$ micro-belts/nickel-coated carbon fibers composites

Bao-Feng Zhao^a, Peixian Ma^{b,c}, Ju-Min Zhao^c, Deng-Ao Li^{c,*}, Xiaoli Yang^d

^aCollege of Mining Engineering, Taiyuan University of Technology, Taiyuan 030024, China

^bThe 33rd Research Institute of China Electronics Technology Group Corporation, 030001, China

^cCollege of Information Engineering, Taiyuan University of Technology, Taiyuan 030024, China

^dDepartment of Electrical and Computer Engineering, Purdue University, Calumet 46323-2094, USA

Received 10 July 2012; received in revised form 26 August 2012; accepted 27 August 2012

Available online 10 September 2012

Abstract

The $\text{Li}_{0.35}\text{Zn}_{0.3}\text{Fe}_{2.35}\text{O}_4$ micro-belts were prepared by cotton template for the first time. The nickel-coated carbon fibers were obtained by the electroless plating method. The formation mechanism of the ferrite micro-belt was studied. The microwave absorption properties of the two layers absorbers containing $\text{Li}_{0.35}\text{Zn}_{0.3}\text{Fe}_{2.35}\text{O}_4$ micro-belts and nickel-coated carbon fibers composites were investigated in the frequency range of 30–6000 MHz. The absorbers of the $\text{Li}_{0.35}\text{Zn}_{0.3}\text{Fe}_{2.35}\text{O}_4$ micro-belts/nickel-coated carbon fibers composites have much better microwave absorption properties than the nickel-coated carbon fibers absorbers, and the microwave absorption properties of the composites are influenced by the content of the absorber.

© 2012 Elsevier Ltd and Techna Group S.r.l. All rights reserved.

Keywords: A. Carbon fiber; B. Directional orientation; B. Magnetic properties; D. Electron microscopy

1. Introduction

With the increasing environmental concern for microwave irradiations and the stealth technology for military platforms, microwave absorbing materials have attracted much attention [1–3]. Generally, they can be classified into single-layer absorber and multi-layer absorber. Sun et al. [4] reported the single-layer absorber containing the hierarchical dendrite-like magnetic materials of Fe_3O_4 , $\gamma\text{-Fe}_2\text{O}_3$, and Fe. Ding et al. [5] investigated the microwave absorbing properties of SiC fiber woven fabrics. Han et al. [6] found that the FeCo/C nano-capsules exhibited the broadband electromagnetic wave absorption. Recently, researchers are interested in double and multi-layer microwave absorbers [7–9], as one layer absorbing materials are usually hard to meet demands simultaneously for wide frequency range and thin absorption layer. The double-layer microwave absorber based on the M-type $\text{BaFe}_{12}\text{O}_{19}$ and W-type $\text{BaCo}_2\text{Fe}_{16}\text{O}_{27}$ ferrites and short carbon fibers were studied by Shen et al. [10]. When the W-type ferrite (60 wt%) was used as the

absorbing layer and the M-type ferrite (60 wt%) composite filled with short carbon fibers (0.2 wt%) was used as the matching layer with the total layer thickness of 2.0 mm, the absorption band width could reach 3.2 GHz where the RL value was below -10 dB, and the minimum RL value was -22.0 dB at about 12.7 GHz. Wang et al. [11] prepared the double-layer microwave absorbers consisting of carbonyl iron (CI) as the matching layer, and carbon black (CB) as the absorbing layer. With 50 wt% of CI and 40 wt% of CB, the minimum RL is about -23.3 dB at 5.3 GHz and the RL value was less than -10 dB in the frequency ranges of 5.1–6.2 GHz and 13.7–15.8 GHz, when both the matching layer thickness and absorption layer thickness were 2.0 mm. Qing et al. [12] investigated the single-layer and double-layer microwave absorbers of BaTiO_3 and carbonyl iron powders with various constituents. The results showed the double-layer absorber with thickness of 1.4 mm, which consisted of the matching layer with 50 wt% BaTiO_3 and the absorbing layer with 60 wt% BaTiO_3 and 20 wt% carbon iron had a much better microwave absorption characteristic than the single-layer absorber, with the absorption band width of 10.8–14.8 GHz ($R_L < -10$ dB) and the minimum R_L of -59 dB at 12.5 GHz.

*Corresponding author.

E-mail address: baofengzhao123@163.com (D.-A. Li).

In the past decades, spinel ferrites have been used as microwave absorbents in various forms due to their light-weight, low cost, and good design flexibility [13,14]. Wu et al. [15] discussed the electromagnetic and microwave absorbing properties of $\text{Ni}_{0.5}\text{Zn}_{0.5}\text{Fe}_2\text{O}_4$ /bamboo charcoal core-shell nanocomposites. Meanwhile, as ferromagnetic metals have a high saturation magnetization and complex permeability, they were studied as microwave absorbers for many years [16–18]. However, the ferromagnetic metals usually have a high electric conductivity and their permeability will drastically decrease at high frequencies due to the eddy current effect induced by microwaves [19]. As the spinel ferrite and ferromagnetic metallic fibers are generally characterized with shape anisotropy, they can be used as the structural and functional materials in various fields. NiCFs and their polymer composites, from both mechanical and electrical point of view have attracted much interest especially for EMI shielding (typical applications are for EMI gaskets) [20–25]. To the best of authors' knowledge, few studies are available dealing with EM properties of NiCF reinforced composites in the microwave range. In the present work, we have reported the electromagnetic characteristics and microwave absorption properties of the belt-like $\text{Li}_{0.35}\text{Zn}_{0.3}\text{Fe}_{2.35}\text{O}_4$ and nickel-coated carbon fibers.

2. Experimental procedure

2.1. The preparation of $\text{Li}_{0.35}\text{Zn}_{0.3}\text{Fe}_{2.35}\text{O}_4$ micro-belts

The detailed process of $\text{Li}_{0.35}\text{Zn}_{0.3}\text{Fe}_{2.35}\text{O}_4$ micro-belts preparation could be described as follows: $\text{Li}(\text{NO}_3)_2$, $\text{Zn}(\text{NO}_3)_2$ and $\text{Fe}(\text{NO}_3)_3 \cdot 9\text{H}_2\text{O}$ (the mole ratio of $\text{Li}^{2+}/\text{Zn}^{2+}/\text{Fe}^{3+}$ were 0.35:0.3:2.35) were dissolved in 200 ml de-ionized water. Then citric acid (the mole ratio of citric acid/metal ion were 1:1) was added to the above mixture. Subsequently, the solution was heated and agitated until the volume was approximately 140 ml to form sol. The sol was dripped onto the prepared dry absorbent cotton. Further, the dipped absorbent cotton was dried for 24 h at room temperature and then dried in a drying cabinet at 70 °C. The dried gels were calcined under 1200 °C for 2 h to obtain $\text{Li}_{0.35}\text{Zn}_{0.3}\text{Fe}_{2.35}\text{O}_4$ micro-belts.

2.2. The preparation of nickel-coated carbon fibers

First, CNFs were cleaned and dispersed in ethanol and deionized water, respectively. This process eliminates the residual metal particles on the surface of CNFs and enhances the interfacial adhesion between the CNFs and metal layers. The pre-treated CNFs were then sensitized and activated in an aqueous solution containing SnCl_2 , PdCl_2 , and HCl for about 5 min. These steps allow the adsorption of colloidal Sn^{2+} and Pd^{2+} on the surfaces of the CNFs. Pd particles function as catalytic nucleation seeds.

In the next step, the activated CNFs were accelerated by immersing them for 3 min in an aqueous solution

containing H_2SO_4 . This procedure helps to remove the Sn^{2+} protecting Pd^{2+} and assists with the deposition of finer Pd particles onto the surface of CNFs.

Finally, the pre-treated and catalyzed CNFs were immersed in a metal plating bath (1 L flask) and stirred with a mechanical stirrer. Ni plating solution consists of $\text{NiCl} \cdot 6\text{H}_2\text{O}$ (20 g/L), $\text{Na-PH}_2\text{O}_2 \cdot 6\text{H}_2\text{O}$ (10 g/L), NH_3Cl (40 g/L) and deionized water. Electroless Ni-P plating was performed with the stirring speed of 300 rpm at 90 °C for 1 min.

The mechanical stirring system was used in order to continuously keep up the good dispersion state during electroless plating. The setup consists of the bath, a temperature controller, a condenser and the mechanical stirrer. At this stage, the density and temperature of the plating solution and the stirring speed of the mechanical stirrer are the most important factors for a uniform deposition of metal onto the surface of the CNFs.

2.3. Measurement of properties

The crystalline structure of the samples was determined by D/max-A diffractometer (Cu $\text{K}\alpha$ radiation, $\lambda = 0.154056$ nm) studies. The morphology of as-prepared samples was investigated by a scanning electron microscope (SEM). The samples for measuring microwave properties were prepared by dispersing the composites powders in paraffin wax. The powder/wax composites were die-pressed to form cylindrical toroidal specimens with 7.0 mm outer diameter, 3.0 mm inner diameter, and 3 mm thickness. The measurements of microwave loss property for the specimens were carried out using a PNA 3629D vector network analyzer in the 30–6000 MHz range.

3. Results and discussion

3.1. Phase analysis and the SEM morphology

The single phase crystalline nature of the belt-like $\text{Li}_{0.35}\text{Zn}_{0.3}\text{Fe}_{2.35}\text{O}_4$ and nickel-coated carbon fibers was confirmed by powder X-ray diffraction. As shown in Fig. 1A, the peak position and relative intensity of all diffraction peaks for the product of $\text{Li}_{0.35}\text{Zn}_{0.3}\text{Fe}_{2.35}\text{O}_4$ match well with the standard powder diffraction data, and no impurity peak is observed, which indicates that high purity crystalline $\text{Li}_{0.35}\text{Zn}_{0.3}\text{Fe}_{2.35}\text{O}_4$ has been synthesized. The (3 1 1) peak was chosen for calculating the average crystalline size. The Scherrer formula analysis shows that the size of the $\text{Li}_{0.35}\text{Zn}_{0.3}\text{Fe}_{2.35}\text{O}_4$ is about 9.0 nm. Fig. 1B shows the XRD pattern of the NCF. The peak at $2\theta = 24.9^\circ$ is the (0 0 2) plane of graphite carbon and the other four peaks at 44.5° , 51.9° , 76.4° and 92.9° correspond to the (1 1 1), (2 0 0), (2 2 0) and (3 1 1) planes of nickel, respectively.

Fig. 2 shows the SEM images of the prepared $\text{Li}_{0.35}\text{Zn}_{0.3}\text{Fe}_{2.35}\text{O}_4$ and nickel-coated carbon fibers. It could be found that the $\text{Li}_{0.35}\text{Zn}_{0.3}\text{Fe}_{2.35}\text{O}_4$ is of belt shape. The thickness of the $\text{Li}_{0.35}\text{Zn}_{0.3}\text{Fe}_{2.35}\text{O}_4$ belt ranges from 1 to 10 μm .

3.2. The formation of the $\text{Li}_{0.35}\text{Zn}_{0.3}\text{Fe}_{2.35}\text{O}_4$ micro-belts

The $\text{Li}_{0.35}\text{Zn}_{0.3}\text{Fe}_{2.35}\text{O}_4$ micro-belts were synthesized. In the formation process of the complex sol, the complex reaction between citric acid and metal ions resulted in the

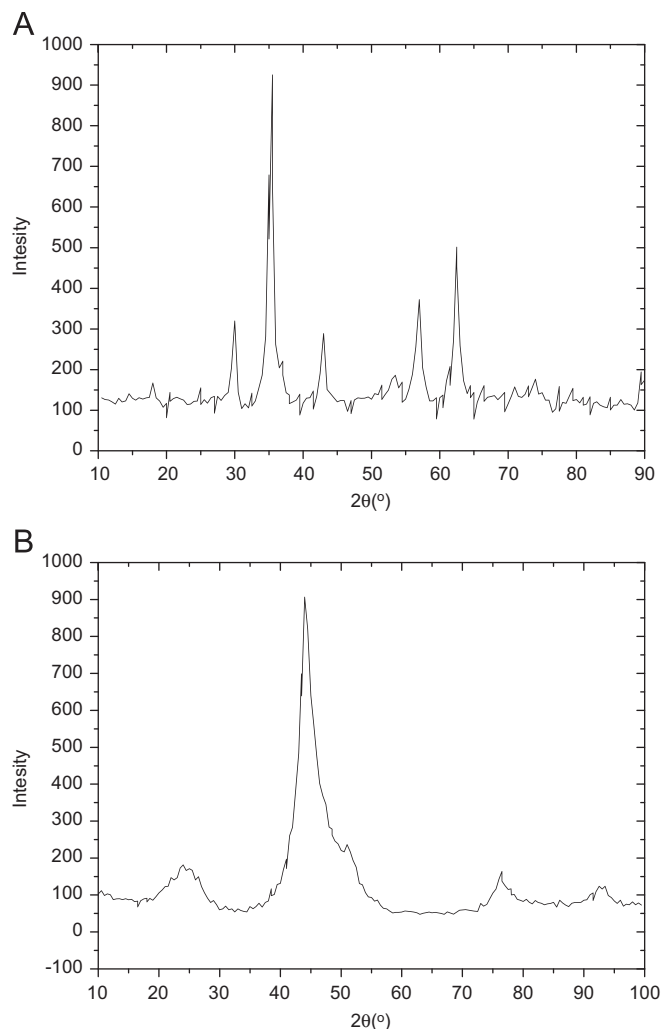


Fig. 1. XRD spectra of samples: (A) belt-like $\text{Li}_{0.35}\text{Zn}_{0.3}\text{Fe}_{2.35}\text{O}_4$; and (B) nickel-coated carbon fibers.

formation of the citric acid complex. This complex was dissolved in distilled water to form sol. When the solution of the citric acid complex was heated, the viscosity of solution increased, thereby forcing the complex molecules to come together. Therefore, the unstable citric acid complex molecules which did not contain the activated function of the condensation–polymerization reaction, underwent cross linking through hydrogen bonds, and resulted in the formation of network structure. Then, when the anions and solvent were embedded into the network structure, gel was formed. Absorbent cotton was used as the template in our experiment. Because the surface of the absorbent cotton was ragged, when the sol was dripped onto the surface of the absorbent cotton, the citric acid complex was absorbed first. On the volatilization of the moisture content in air, hydrogen bonds formed between this complex and the $-\text{OH}$ on the absorbent cotton surface. Due to the evaporation of the moisture content, the excessive active groups in citric acid complex combined with each other through hydrogen bonds. With the process of the polymerization reaction of the system, the thickness of the $\text{Li}_{0.35}\text{Zn}_{0.3}\text{Fe}_{2.35}\text{O}_4$ layer increases. In the dry process, both $\text{Li}_{0.35}\text{Zn}_{0.3}\text{Fe}_{2.35}\text{O}_4$ layer and the cotton fiber shrunk with the decrease of the solvent. However, the shrinkage ratios of the $\text{Li}_{0.35}\text{Zn}_{0.3}\text{Fe}_{2.35}\text{O}_4$ layer and the cotton fiber are different. Thus, the crack phenomena appear on the surface of the $\text{Li}_{0.35}\text{Zn}_{0.3}\text{Fe}_{2.35}\text{O}_4$ layer. The crack swells with decrease in the amount of the solvent. In the calcination process, there exists a large impulse force on the $\text{Li}_{0.35}\text{Zn}_{0.3}\text{Fe}_{2.35}\text{O}_4$ layer for the combustion of cotton fiber. Thus, the $\text{Li}_{0.35}\text{Zn}_{0.3}\text{Fe}_{2.35}\text{O}_4$ layer breaks along the crack, and the $\text{Li}_{0.35}\text{Zn}_{0.3}\text{Fe}_{2.35}\text{O}_4$ belts are obtained. The detailed formation mechanism of belt-like $\text{Li}_{0.35}\text{Zn}_{0.3}\text{Fe}_{2.35}\text{O}_4$ is shown in Fig. 3. The mechanism of the $\text{Li}_{0.35}\text{Zn}_{0.3}\text{Fe}_{2.35}\text{O}_4$ microbelt formation is still not clear, and should be extensively studied in the future.

3.3. Analysis of electromagnetic parameters and wave absorbing property

The frequency dependences of the complex permeability and permittivity of $\text{Li}_{0.35}\text{Zn}_{0.3}\text{Fe}_{2.35}\text{O}_4$ microbelt and

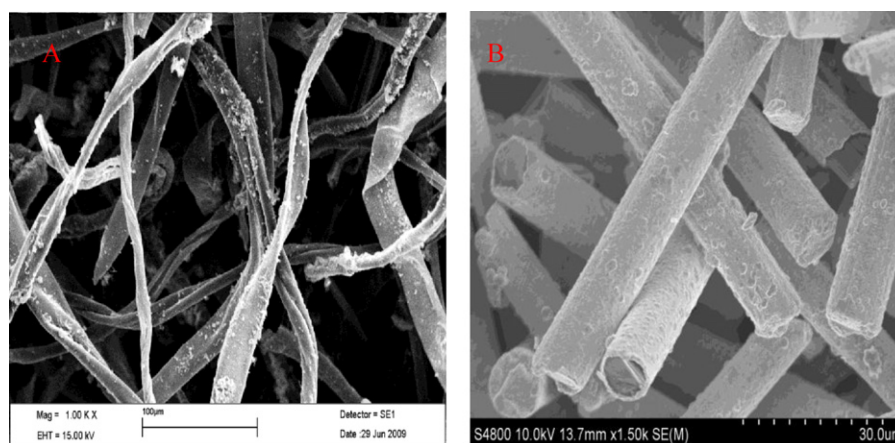


Fig. 2. The SEM images of the samples: (A) belt-like $\text{Li}_{0.35}\text{Zn}_{0.3}\text{Fe}_{2.35}\text{O}_4$; and (B) nickel-coated carbon fibers.

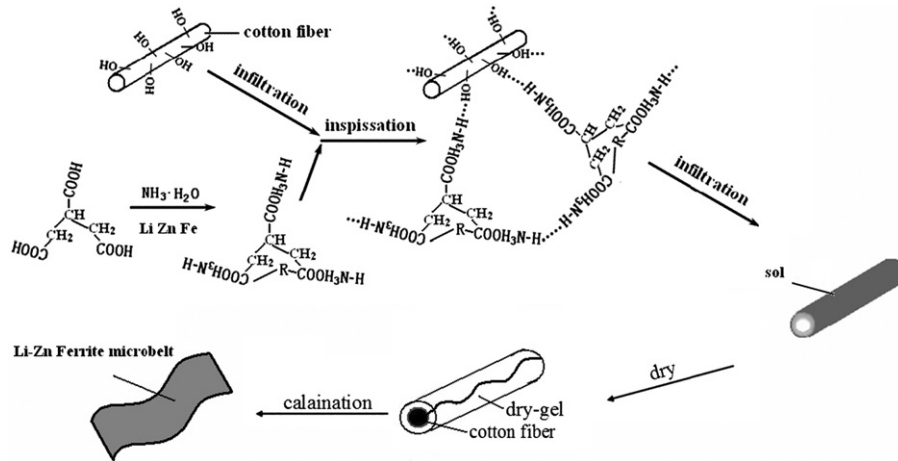


Fig. 3. The formation mechanism of belt-like $\text{Li}_{0.35}\text{Zn}_{0.3}\text{Fe}_{2.35}\text{O}_4$. (R:Li, Fe, or Zn).

nickel-coated carbon fibers microwave absorber are shown in Figs. 4 and 5, respectively. From Fig. 4, it can be found that, the “ ϵ_r ” of the $\text{Li}_{0.35}\text{Zn}_{0.3}\text{Fe}_{2.35}\text{O}_4$ microbelt increases with the increase in frequency. And the resonance peak appears in the curves. This could be due to the loss process during the oscillation of the dipoles under the influence of the TEM wave that dominates in the high-frequency regime. Ref. [20] reported that the dielectric loss presents different loss mechanisms as the frequency increases. When the frequency is relatively low, the loss is determined by the leak conductance and the loss is independent of the frequency. As the frequency increases to microwave frequency band, the mechanisms are relaxation polarization loss and electric conductance loss. The increase in the imaginary component of the permittivity as the frequency increases may be the consequence of the increase of the relaxation polarization loss and the electric conductance loss.

The complex permittivity for the $\text{Li}_{0.35}\text{Zn}_{0.3}\text{Fe}_{2.35}\text{O}_4$ microbelt and nickel-coated carbon fibers microwave absorber is shown in Fig. 5. The imaginary part “ μ_r ” of the complex permittivity increases with increasing frequency. The imaginary part “ μ_r ” of the complex permittivity for $\text{Li}_{0.35}\text{Zn}_{0.3}\text{Fe}_{2.35}\text{O}_4$ microbelt is higher than that of the nickel-coated carbon fibers (especially in the 3–4 GHz). This is because the $\text{Li}_{0.35}\text{Zn}_{0.3}\text{Fe}_{2.35}\text{O}_4$ microbelt is a micropore-like magnetic material. Thus the magnetic loss of micro-pore structure is larger.

Electromagnetic parameters (μ' , μ'' , ϵ' , ϵ'') are the intrinsic features of absorbing materials. The normalized input impedance (Z) with respect to the impedance in free space, and reflection loss (R_L) are given by

$$Z = \sqrt{\frac{\mu_r}{\epsilon_r}} \tanh \left[-j \left(\frac{2\pi}{c} \right) (\sqrt{\mu_r \epsilon_r}) f d \right]$$

$$R_L(\text{dB}) = -20 \log \left[\left| \frac{(Z-1)}{(Z+1)} \right| \right]$$

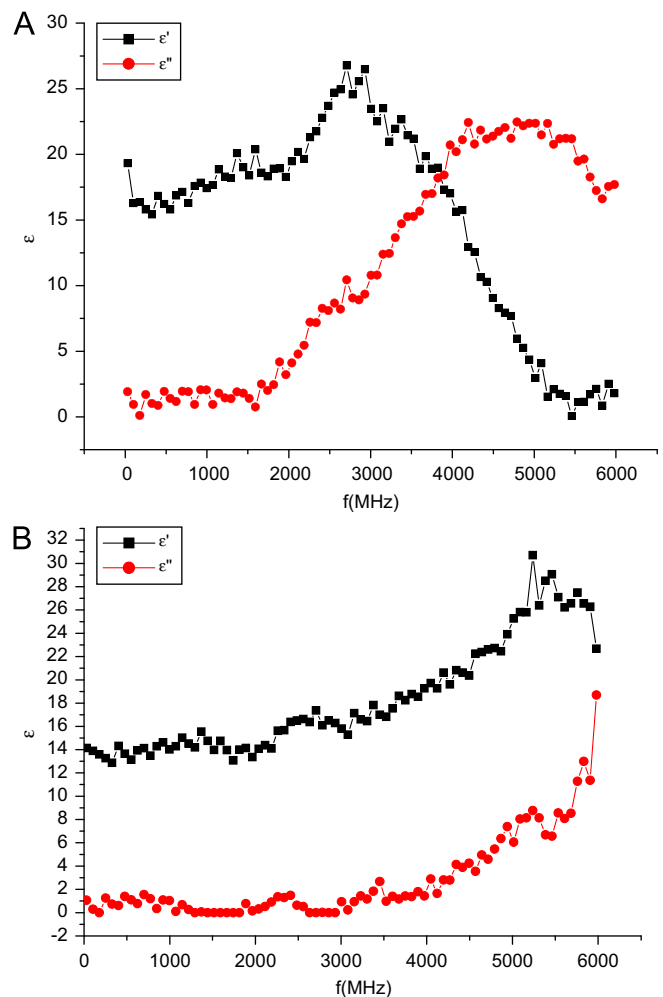


Fig. 4. Frequency dependences of the complex permittivity of samples: (A) belt-like $\text{Li}_{0.35}\text{Zn}_{0.3}\text{Fe}_{2.35}\text{O}_4$; and (B) nickel-coated carbon fibers.

where μ_r and ϵ_r are the relative complex permeability and permittivity of the absorber medium, respectively, f and c are respectively, the frequency of microwave in free space and the velocity of light, and d is the sample thickness.

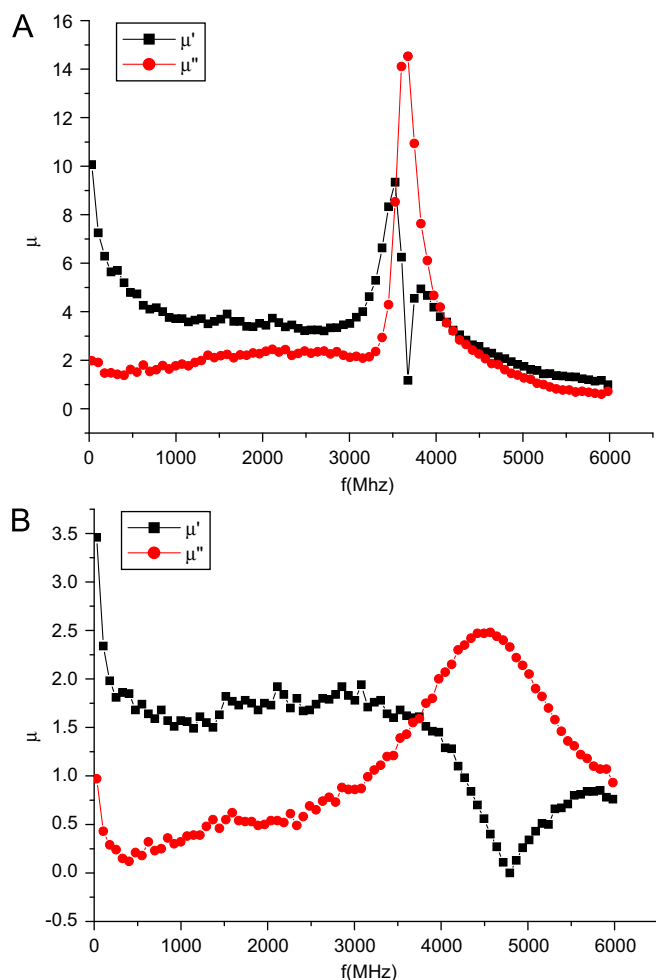


Fig. 5. Frequency dependences of the complex permeability of samples: (A) belt-like $\text{Li}_{0.35}\text{Zn}_{0.3}\text{Fe}_{2.35}\text{O}_4$; and (B) nickel-coated carbon fibers.

Fig. 6 shows the calculated reflection loss as a function of frequency for samples. The microwave absorbance of the samples can be predicted from R_L in which the larger the negative value of R_L , the greater the microwave absorption properties of materials. The most important and interesting observation is that the reflection loss is found to depend sensitively on the content of $\text{Li}_{0.35}\text{Zn}_{0.3}\text{Fe}_{2.35}\text{O}_4$ micro-belts absorber. For the sample F, the microwave absorbance of the sample in the frequency bands is very low. For the sample A,B,C, the microwave absorbance of the sample increases with the increasing content of the $\text{Li}_{0.35}\text{Zn}_{0.3}\text{Fe}_{2.35}\text{O}_4$ microbelt in the composites. And the resonance peak of the composites can be adjusted to lower frequency band by adjusting the content of the $\text{Li}_{0.35}\text{Zn}_{0.3}\text{Fe}_{2.35}\text{O}_4$ microbelt. And the band width below -5 dB increased with the increase in the $\text{Li}_{0.35}\text{Zn}_{0.3}\text{Fe}_{2.35}\text{O}_4$ content. When the content of the nickel-coated carbon fibers is higher than 40%, the resonance peak of the composites lies in the lower frequency. However the negative of the R_L is lower than the samples A, B and C. This is because the higher ratio of nickel-coated carbon fibers results in the strong reflex phenomenon of the incident microwave. The variation of reflection loss results

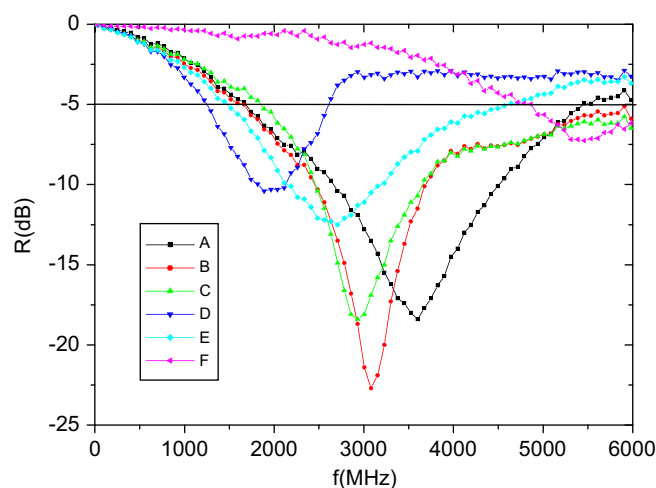


Fig. 6. Microwave-absorbing properties of samples: (A) NiCF(25%)+Ferrite(40%), 5 mm; (B) NiCF(25%)+Ferrite(50%), 5 mm; (C) NiCF(25%)+Ferrite(60%), 5 mm; (D) NiCF(40%)+Ferrite(40%), 5 mm; (E) NiCF(40%)+Ferrite(50%), 5 mm and (F) NiCF(25%), 5 mm.

of the samples is coherent with the variation of the complex permeability and permeability (Figs. 4 and 5) of the sample as the formulas above. The band width below -5 dB of the sample B is up to 3336 MHz. The structure of the $\text{Li}_{0.35}\text{Zn}_{0.3}\text{Fe}_{2.35}\text{O}_4$ microbelt has an effect on the microwave absorption behavior of the composites.

4. Conclusions

The $\text{Li}_{0.35}\text{Zn}_{0.3}\text{Fe}_{2.35}\text{O}_4$ micro-belts were prepared by cotton template for the first time. The nickel-coated carbon fibers were obtained by the electroless plating method. The formation mechanism of the ferrite micro-belt was studied. The microwave absorption properties of the $\text{Li}_{0.35}\text{Zn}_{0.3}\text{Fe}_{2.35}\text{O}_4$ micro-belts/nickel-coated carbon fibers composites were investigated in the frequency range of 30–6000 MHz. The absorbers of the $\text{Li}_{0.35}\text{Zn}_{0.3}\text{Fe}_{2.35}\text{O}_4$ micro-belts/nickel-coated carbon fibers composites have much better microwave absorption properties than the nickel-coated carbon fibers absorbers, and the microwave absorption properties of the composites are influenced by the content of the absorber. The structure of the $\text{Li}_{0.35}\text{Zn}_{0.3}\text{Fe}_{2.35}\text{O}_4$ microbelt has an effect on the microwave absorption behavior of the composites.

Declaration

The article is original, has been written by the stated authors who are all aware of its content and approve its submission, has not been published previously, it is not under consideration for publication elsewhere, no conflict of interest exists, or if such conflict exists, the exact nature of the conflict must be declared and if accepted, the article will not be published elsewhere in the same form, in any language, without the written consent of the publisher.

Acknowledgments

This paper is funded by the Shanxi University Science & Technology Project (20090011), the Shanxi Youth Science Foundation (2010021017-1), the Shanxi Science and Technology Development Plan (Industrial Sector) (20120321024-01) and the Shanxi Province International Scientific and Technological Cooperation Project (2012081031).

References

- [1] S.S. Kim, D.H. Han, S.B. Cho, Microwave absorbing properties of sintered Ni–Zn ferrite, *IEEE Transactions on Magnetics* 30 (1994) 4554–4556.
- [2] Y.L. Yang, M.C. Gupta, K.L. Dudley, R.W. Lawrence, Novel carbon nanotube–polystyrene foam composites for electromagnetic interference shielding, *Nano Letters* 5 (2005) 2131–2134.
- [3] X.Z. Zhang, W. Sun, Microwave absorbing properties of double-layer cementitious composites containing Mn–Zn ferrite, *Cement and Concrete Composites* 32 (2010) 726–730.
- [4] G.B. Sun, B.X. Dong, M.H. Cao, B.Q. Wei, C.H. Hu, Hierarchical dendrite-like magnetic materials of Fe_3O_4 , $\text{c-Fe}_2\text{O}_3$, and Fe with high performance of microwave absorption 23 (2011) 1587–1593 *Chemistry of Materials* 23 (2011) 1587–1593.
- [5] D.H. Ding, W.C. Zhou, B. Zhang, F. Luo, D.M. Zhu, Complex permittivity and microwave absorbing properties of SiC fiber woven fabrics, *Journal of Materials Science* 46 (2011) 2709–2714.
- [6] Z. Han, D. Li, H. Wang, X.G. Liu, J. Li, D.Y. Geng, et al., Broadband electromagnetic wave absorption by FeCo/C nanocapsules, *Applied Physics Letters* 951 (2009) 023114.
- [7] Y.B. Feng, T. Qiu, C.Y. Shen, Absorbing properties and structural design of microwave absorbers based on carbonyl iron and barium ferrite, *Journal of Magnetism and Magnetic Materials* 318 (2007) 8–13.
- [8] Z.Q. Liao, Y. Nie, W.Y. Ren, X. Wang, R.Z. Gong, Effect of FeCoB– SiO_2 -film-based fractal frequency selective surface on the absorption properties of microwave absorbers, *IEEE Magnetics Letters* 1 (2010) 5000204.
- [9] M.X. Chen, Y. Zhu, Y.B. Pan, H.M. Kou, H. Xu, J.K. Guo, Gradient multilayer structural design of CNTs/ SiO_2 composites for improving microwave absorbing properties, *Materials and Design* 32 (2011) 3013–3016.
- [10] G.Z. Shen, M. Xu, Z. Xu, Double-layer microwave absorber based on ferrite and short carbon fiber composites, *Materials Chemistry and Physics* 105 (2007) 268–272.
- [11] M. Wang, Y.P. Duan, S.H. Liu, X.G. Li, Z.J. Ji, Absorption properties of carbonyl-iron/carbon black double-layer microwave absorbers, *Journal of Magnetism and Magnetic Materials* 321 (2009) 3442–3446.
- [12] Y.C. Qing, W.C. Zhou, F. Luo, D.M. Zhu, Optimization of electromagnetic matching of carbonyl iron/ BaTiO_3 composites for microwave absorption, *Journal of Magnetism and Magnetic Materials* 323 (2011) 600–606.
- [13] C.H. Peng, C.C. Hwang, J. Wan, J.S. Tsai, S.Y. Chen, Microwave-absorbing characteristics for the composites of thermal-plastic polyurethane (TPU)-bonded NiZn-ferrites prepared by combustion synthesis method, *Materials Science and Engineering B* 117 (2005) 27–36.
- [14] Y. Hwang, Microwave absorbing properties of NiZn-ferrite synthesized from waste iron oxide catalyst, *Materials Letters* 60 (2006) 3277–3280.
- [15] K.H. Wu, T.H. Ting, C.I. Liu, C.C. Yang, J.S. Hsu, Electromagnetic and microwave absorbing properties of $\text{Ni}_{0.5}\text{Zn}_{0.5}\text{Fe}_2\text{O}_4$ /bamboo charcoal core–shell nanocomposites, *Composites Science and Technology* 68 (2008) 132–139.
- [16] J.R. Liu, M. Itoh, K.I. Machida, GHz range absorption properties of a Fe/ Y_2O_3 nanocomposites prepared by melt–spun technique, *Chemistry Letters* 4 (2003) 394–395.
- [17] X.F. Zhang, X.L. Dong, H. Huang, Y.Y. Liu, B. Lv, J.P. Lei, et al., Microstructure and microwave absorption properties of carbon-coated iron nanocapsules, *Journal of Physics D: Applied Physics* 40 (2007) 5383–5387.
- [18] J.R. Liu, M. Itoh, M. Terada, T. Horikawa, K. Machida, Enhanced electromagnetic wave absorption properties of Fe nanowires in gigahertz range, *Applied Physics Letters* 91 (2007) 093101.
- [19] D. Rousselle, A. Berthault, O. Acher, J.P. Bouchaud, P.G. Zerah, Effective medium at finite frequency: theory and experiment, *Journal of Applied Physics* 74 (1993) 475–479.
- [20] V. Di Liello, E. Martuscelli, G. Ragosta, A. Zihlif, Tensile properties and fracture behaviour of polypropylene–nickel-coated carbon–fibre composite, *Journal of Materials Science* 25 (1) (1990) 706–712.
- [21] M.S. Ahmad, M.K. Abdelazeez, A. Zihlif, E. Martuscelli, G. Ragosta, E. Scafara, Some properties of nickel-coated carbon fibre–polypropylene composite at microwave frequencies, *Journal of Materials Science* 25 (7) (1990) 3083–3088.
- [22] M.S. Ahmad, A.M. Zihlif, E. Martuscelli, G. Ragosta, E. Scafara, The electrical conductivity of polypropylene and nickel-coated carbon fiber composite, *Polymer Composites* 13 (1) (1992) 53–57.
- [23] X. Shui, D.D.L. Chung, Submicron nickel filaments made by electroplating carbon filaments as a new filler material for electromagnetic interference shielding, *Journal of Electronic Materials* 24 (2) (1995) 107–113.
- [24] G. Lu, X. Li, H. Jiang, Electrical and shielding properties of ABS resin filled with nickel-coated carbon fibers, *Composites Science and Technology* 56 (2) (1996) 193–200.
- [25] X. Shui, D.D.L. Chung, Submicron diameter nickel filaments and their polymer–matrix composites, *Journal of Materials Science* 35 (7) (2000) 1773–1785.